Bull. Mater. Sci., Vol. 33, No. 1, February 2010, pp. 55–63. © Indian Academy of Sciences.

Function of magnesium aluminate hydrate and magnesium nitrate as MgO addition in crystal structure and grain size control of α-Al_2O_3 during sintering

SOUMEN PAL*, A K BANDYOPADHYAY, S MUKHERJEE[†], B N SAMADDAR[††] and P G PAL

Department of Ceramic Technology, Government College of Engineering and Ceramic Technology, Kolkata 700 010, India

[†]School of Material Science and Technology, [††]Department of Metallurgical and Material Engineering, Jadavpur University, Kolkata 700 032, India

MS received 25 November 2008; revised 29 January 2009

Abstract. **Chemically pure reactive alumina (α-Al_2O_3) which is commercially available was used for densification study in presence of widely accepted dopant MgO as additive. MgO was added both as spinel ($MgAl_2O_4$) forming precursor i.e. magnesium aluminate hydrate, and magnesium nitrate. Sintering investigations were conducted in the temperature range 1500–1600°C with 2 h soaking. Structural study of sintered pellets was carried out by extensive XRD analysis. Scanning electron mode SEM images of the specimens were considered to understand the effect of both types of additions. Addition of MgO within and beyond optimum amount had some effect on development of microstructure of sintered bodies. Densification, around 99% ρ_{th}, with fine grain microstructure was achieved. These different types of additions caused two distinct changes in crystal structure of alumina—one small contraction and the other expansion of unit cell parameters.**

Keywords. **Sintering; X-ray methods; electron microscopy; grain growth; solid solubility.**

1. Introduction

Aluminium oxide is a unique ceramic material used for both conventional and advanced applications. Its densification and microstructure control are closely interrelated. These are dependent on characterization of precursor alumina powders i.e. chemistry, particle size, shape and distribution, etc and also on the nature of dopants, their amount and distribution. Some additives have positive role, some negative and a few others remain inert during sintering of alumina in terms of densification and grain growth (Smothers and Reynolds 1954; Cahoon and Christerson 1956). It is reported (Haroun and Budworth 1970) that grain growth and grain shape of nearly full dense alumina, sintered at 1675°C in oxygen atmosphere gets significantly influenced by the particle size of the additives as compared to their chemical nature. Further, volatility of MgO at 1770°C in vacuum helps densification of alumina to its ρ_{th} value when Linde-A alumina pellet is placed between two compacts of analar MgO, and there is formation of $MgAl_2O_4$ on the end layers of Linde-A alumina pellet (Warman and Budworth 1967).

Work of Coble (1961, 1962) opened a new chapter more than four decades ago in alumina research in presence of MgO. Positive effect of MgO addition (Jorgensen and Westbrook 1964; Jorgensen 1965; Taylor *et al* 1974, 1976; Johnson and Coble 1978) in alumina sintering is accompanied by its solid solution in alumina, and excess addition of MgO beyond its solid solubility limit exists as non-stoichiometric spinel in grain boundaries of sintered alumina. Li and Kingery (1984) reported segregation of magnesium aluminate spinel as second phase discrete particles with definite contact angle and no continuous second phase along grain boundaries of alumina, while investigating scanning transmission electron microscopy of MgO doped (0·2–0·5 wt% MgO) alumina sintered at 1575°C for 96 h in oxygen and quenched in liquid nitrogen. Paul and Samaddar (1985) used magnesium aluminate hydrate (MAH) as source of dopant in sintering of commercially available laboratory developed submicron (0·3–0·4 μm) alumina powder of moderate purity (Al_2O_3–99·6 wt%, loss free basis), and showed a trend of lattice contraction of unit cell of alumina as compared to its unit cell expansion in presence of MgO added as magnesium nitrate (MN). They also achieved near ρ_{th} density when addition of MgO (as MAH or MN) was within the solid solubility limit.

*Author for correspondence (soumenpal12@gmail.com)

In the present investigation, the work of Paul and Samaddar (1985) has been extended further with much purer alumina (~99·9 wt% Al_2O_3, loss free basis) as material for investigation. This work includes addition of MgO both as MAH and MN up to 1·13 wt%, and sintering study from 1500–1600°C with 2 h soaking. Sintered bulk density (BD), % apparent porosity (%AP), % true porosity (%TP) and % closed pores (%CP) have been measured at each of the sintering temperatures 1500, 1550 and 1600°C. Densification rate (DR) with addition of MgO (MAH and MN) has been calculated for the sintered pellets to evaluate how mode of addition of MgO in both the forms affects the densification process. Along with the above properties, interpretation of the XRD results and SEM microphotographs generated major motivation for the present work.

2. Experimental

2.1 *Characterization of alumina powder and MAH*

High purity commercial calcined alumina powder (Almatis, USA) was used as base material. For doping alumina with MAH as wt% MgO, the hydrate was prepared from analytical reagent (AR) quality (E-Merck, Germany) magnesium chloride and aluminium sulphate mix solution by co-precipitation technique (Mukherjee and Samaddar 1969; Samaddar *et al* 1979) using liquor ammonia as precipitating agent. Concentration of mixed salt solution, reaction temperature and pH during co-precipitation were closely controlled so that the co-precipitated material on further processing (drying and calcination) gave stoichiometric magnesium aluminate spinel. Also, same AR grade magnesium nitrate was taken in case of doping alumina with MN as wt% MgO.

Conventional wet chemical method (WCM) was used to estimate Al_2O_3, SiO_2, Fe_2O_3, MgO and CaO present in dried (110°C, 24 h) powder on loss free basis. Na_2O was estimated by Flame Photometer. Phases present in the dried powder were studied by XRD analysis. Particle size distribution was measured in Sedigraph (Sedigraph–III 5120, Micromeritics, USA) by using sodium hexametaphosphate as dispersing agent with X-ray monitored gravity sedimentation technique. To measure solid content of MAH gel like material, around 10 g of it was taken in a pre-weighted Petri dish and dried at 110°C until constant weight and drying loss were calculated. The dried material was agated, again dried at 110°C for 24 h and loss on ignition was found out at 1200°C with 2 h soaking. Same WCM was followed to estimate alumina and magnesia present in MAH and subsequently molar ratio of MgO : Al_2O_3 in MAH was estimated.

2.2 *Batch preparation*

Incorporation of MAH gel in alumina was done based on solid content i.e. 8·35 wt%, after combined weight loss (drying + calcination at 1200°C, 2 h) and also from chemical analysis of the solid (MgO–28·44 wt% and Al_2O_3–71·52 wt%, on loss free basis) to evolve compositions viz. 0·1, 0·2, 0·28, 0·57, 0·85 and 1·13 wt% MgO in alumina. Identical compositions in terms of MgO content were prepared when MN was considered. For better mixing, each batch was shaken vigorously for 45 min in a 500 ml polythene container in presence of measured amount of ethyl alcohol and sintered alumina balls. Each batch was dried at 110°C, agated, calcined at 600°C for 2 h and further agated for homogenization of MgO in alumina.

To understand the difference in loss free basis green BD values between MAH and MN doped samples (listed in table 2), a small amount of 110°C dried MAH powder was calcined at 600°C for 2 h, and then further calcined at 1500°C for 2 h. Thereafter, loss of ignition (LOI) for the MAH powder from 600–1500°C was calculated to be 48·5 wt%. However, for the MN powder the L.O.I from 600–1500°C was negligible. Due to this wt loss of MAH powder, at higher addition of MAH (for 0·57, 0·85 and 1·13 wt% equivalent MgO), there is significant difference in loss free basis green BD values in comparison with MN types (table 2). It is to be noted that as all the batches of both MAH and MN types are already calcined at 600°C, the above L.O.I comparison has been done from

Table 1. Particle size distribution of calcined technical alumina powder (report by mass %).

Low diameter (μm)	Cumulative mass finer (%)
1·209	90
0·735	80
0·583	70
0·491	60
0·421	50
0·361	40
0·305	30
0·245	20
0·176	10

Table 2. Comparison of green BD (loss free basis) when MgO is added as MAH and MN.

Composition (wt% addition of MgO)	True specific gravity	Green BD (MAH)	Green BD (MN)
0·00	3·987	2·14	2·14
0·10	3·986	2·12	2·13
0·20	3·984	2·13	2·15
0·28	3·983	2·22	2·20
0·57	3·979	2·15	2·22
0·84	3·975	2·08	2·22
1·13	3·971	2·02	2·23

600–1500°C. As the sintering temperatures of the pellets are at 1500, 1550 and 1600°C, selection of 1500°C to calculate the L.O.I of MAH and MN materials is justified because beyond 1500°C the loss would have been nil or negligible.

High carbon steel mould of internal diameter, 2·55 cm, was used to prepare cylindrical pellets in a hydraulic press at 1550 kg/cm^2 forming pressure. Thickness of the green pellets was maintained at ~6 mm. From dimensions and mass, green density of the pellets was calculated (8 pellets for each composition).

2.3 *Sintering and measurement of physical properties of sintered pellets*

Three sintering temperatures, 1500, 1550 and 1600°C, were selected for all batch compositions. Two pellets of each composition were fired in an electrically heated muffle furnace (Bysakh & Co, India) with a heating schedule of 8°C/min up to 1200°C, and then 5°C/min up to respective firing temperature with 2 h soaking. Forced cooling was done up to 800°C with exhaust fan attached to the furnace, and afterwards normal cooling up to room temperature. Conventional boiling method was used to measure BD, %AP and apparent specific gravity of the sintered pellets. In each case, average value of the two pellets had been considered. For measurement of %TP and %CP, true specific gravity of the sintered samples (i.e. after fine agating to –300 BS sieve) was measured with specific gravity bottles using xylene.

2.4 *XRD and SEM*

XRD (Miniflex, Rigaku, Japan) was used for analysis of sintered pellets, both doped and un-doped, using Cu as target and operated at 30 kV, 15 mA. Goniometer speed was 1°/min and scanned from 15–75°. From XRD of the sintered tablets, *d*-values of major peaks of α-Al_2O_3 were used for calculation of unit cell parameters '*a*' and '*c*', and unit cell volume of alumina. SEM (JSM 6360, JEOL, Japan) was conducted on palladium coated fractured surfaces of sintered pellets (1600°C, 2 h). Snaps were recorded on scanning electron mode and the operational voltage of SEM was kept at 20 kV.

3. Results and discussion

3.1 *Characterization of alumina powder*

Chemical analysis of alumina powder (Al_2O_3–99·86 wt%, Na_2O–0·018 wt%, Fe_2O_3–0·015 wt%, CaO + MgO–0·009 wt%, SiO_2–0·012 wt%) indicates that very low amount of impurities (~0·1 wt%) may have little effect on the role, which MgO plays on the unit cell parameters of alumina, during sintering. Particle size distribution (table 1) of alumina reveals that most part of the powder is in submicron level, and around 87 wt% of the material in the range 1 μm to 100 nm (in table 1, cumulative % values at an interval of 10 have been listed as the total data set is quite voluminous). This fineness in size confirms the sinter-active nature of the powder at the firing temperatures 1500, 1550 and 1600°C. Both chemistry and true specific gravity (i.e. 3·987) of the alumina powder indicate that it consists of only α-alumina, which was also confirmed by XRD.

3.2 *Sintering and densification*

Green density (loss free basis) along with true specific gravity of samples, having different wt% MgO, have been incorporated in table 2. Negative trend of green BD (loss free basis) was observed when addition of MAH (wt% equivalent MgO) was beyond certain percent. As already mentioned, the mixture of MAH gel and alumina powder was calcined at 600°C. During calcination at 600°C, the MAH does not decompose completely and remains in between alumina particles forming agglomerates of alumina particles. This agglomeration is high when MAH addition is more (beyond 0·28 wt% MgO equivalent). Due to this agglomeration, there is slight decrease in green BD at 0·57, 0·85 and 1·13 wt% MgO equivalent MAH additions. However, for MN type of samples, this type of phenomenon hardly occurs as most of the magnesium nitrate decomposes during calcination at 600°C. Also there is a significant wt loss of MAH powder from 600–1500°C (discussed in §2.2). Therefore, the green BD for MAH type of samples is less when compared with MN types at 0·57, 0·85 and 1·13 wt% addition of MgO. Measured values of sintered BD, %AP, %TP and %CP at each sintering temperature, viz. 1500, 1550 and 1600°C, are graphically correlated with wt% addition of MgO as MAH and MN.

Figure 1 reveals the change of BD of sintered alumina pellets with wt% addition of MgO in both the forms at 1500, 1550 and 1600°C with 2 h soaking. At 1500°C, addition of MgO has less effect in improvement of sintered density of alumina. There is a slight negative effect with addition of 0·1 wt% MgO in both MAH and MN. Improvement of sintered density takes place at 0·2 wt% addition of MgO for both types of additions. Positive effect of MgO addition continues up to 0·57 wt% in case of MAH. However, further addition of MgO (as MAH) reduces the density of alumina. At 1550°C, improvement of sintered density of alumina continues up to 0·57 wt% MgO addition in both the cases (it is maximum at 0·28 wt% in case of MAH). But addition of MgO gives better densification when added as MAH than MN till 0·85 wt%. Higher wt% MgO addition retards the densification process particularly when added in the form of

MAH. At 1600°C, MgO addition as MN has largely negative effect on sintering of alumina in comparison with MAH. The overall sintering behaviour of alumina explains that densification mechanisms are different for both types of additions of MgO.

%AP of sintered alumina (figure 2) gives entirely different picture when addition of MgO is in the form of MN. %AP is always lower for each amount of MgO addition as MN when compared with MAH. This reverse trend of BD with %AP indicates that sintered pellets have more %CP when addition of MgO is in the form of MN. One inference which can be derived from this behaviour is that existence of %CP will help abnormal grain growth of sintered pellets. Measurement of %TP (figure 3) of sintered pellets establishes that MgO addition as MAH gives a lower value when compared with MN.

Presence of %CP (figure 4) is more prominent in sintered pellets which contain MgO added as MN at all sintering temperatures. Comparison of the curves in figure 4 indicates that MgO addition as MAH is more effective to reduce secondary grain growth of alumina as because extent of pore entrapment is lower. Minimum %CP in the present investigation (0·87, 1·22 and 1·26% at 1500, 1550 and 1600°C, respectively for MAH doped as compared to 3·04, 2·49 and 2·92% at 1500, 1550 and 1600°C, respectively for MN doped) indicates that MAH is more effec-

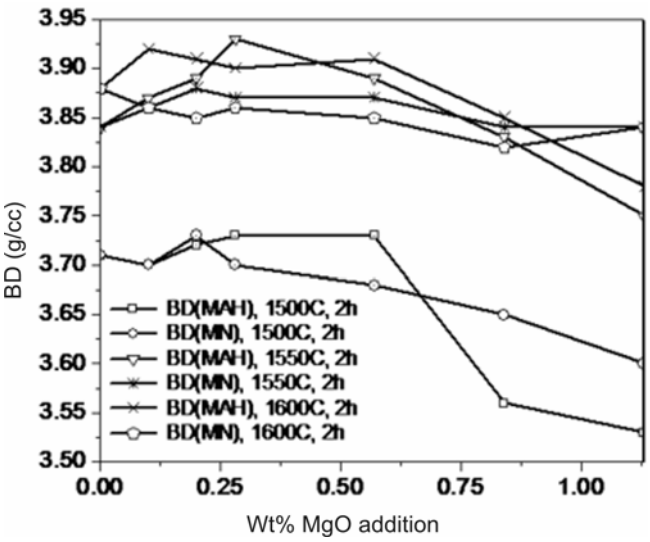

Figure 1. Effect of MgO addition as MAH/MN on bulk density (BD) of sintered alumina.

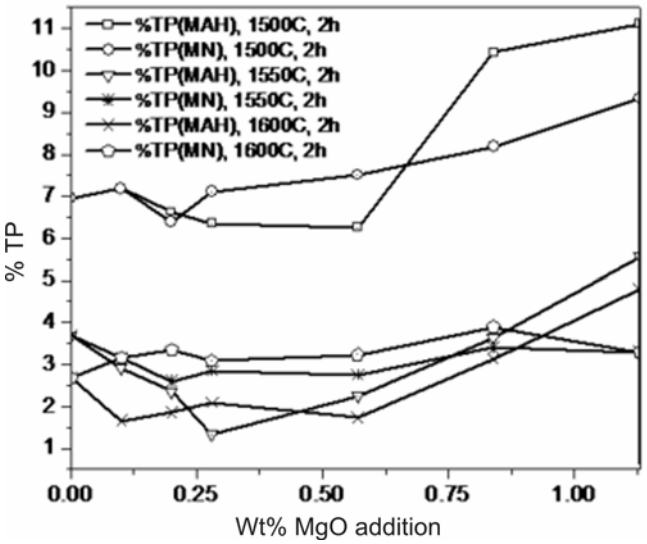

Figure 3. Effect of MgO addition as MAH/MN on %TP of sintered alumina.

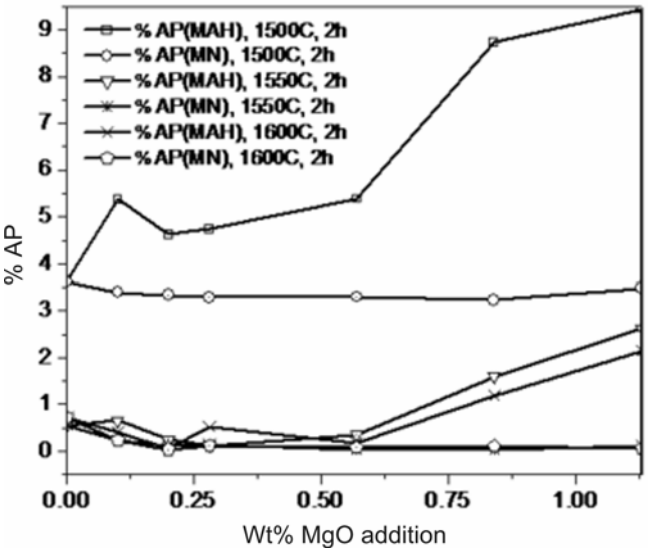

Figure 2. Effect of MgO addition as MAH/MN on %AP of sintered alumina.

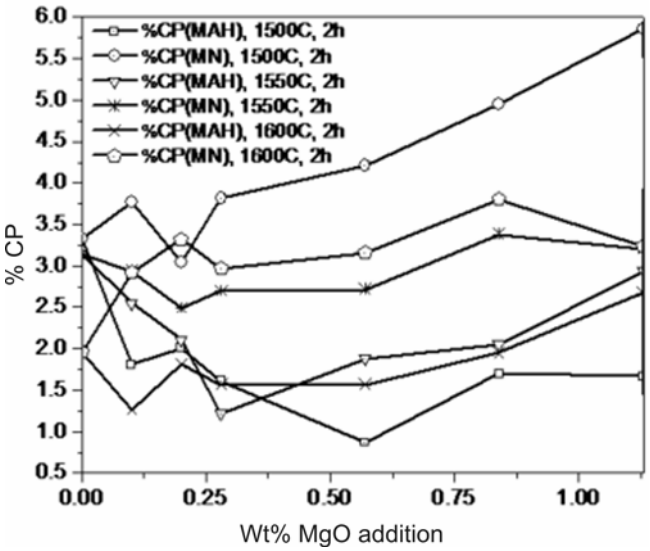

Figure 4. Effect of MgO addition as MAH/MN on %CP of sintered alumina.

tive as source of MgO addition than MN for densification of alumina bodies. Cohen *et al* (1984) studied the effect of dopant (MgO) dispersion in alumina on density, %AP and closed pores of sintered alumina at 1500, 1550 and 1600°C up to 2 h and reported the presence of higher %CP (9·8–22·7%) which hindered densification process during sintering.

During sintering, mass of the pellets is assumed not to change. As pre-calcined (600°C, 2 h) MAH undergoes 48·5 wt% L.O.I, this reduces the green BD of the pellets when calculated by loss free basis. Effectiveness of both types of MgO additions in sintering of alumina can be expressed as densification rate (DR) with respect to green density (loss free basis) by using the formula

$$\frac{\text{Sintered BD} - \text{Green BD}}{\text{Green BD}} \times 100.$$

These results have been incorporated in figure 5. DR increases up to 0·2 wt% addition of MgO either as MAH or MN. Beyond 0·2 wt% of MgO, it decreases with increasing proportion of MgO added as MN at all temperatures. The trend is different in case of MgO addition as MAH where the rate reaches a minimum at 0·28 wt% MgO, and later the value increases with higher proportion of MgO. It can be seen as an example that at 1·13 wt% MgO addition, the green BD (loss free basis) for MAH and MN types are 2·02 and 2·23, respectively. But DR at 1600°C, 2 h for MAH type is more compared to MN type although sintered BD value at this particular composition of MN sample is greater than MAH doped pellet (figure 1).

The present work reveals that not only amount of MgO addition but also its nature plays some role to achieve maximum density during sintering. Beyond powder granulometry, amount and nature of MgO additions; other parameters like forming process, firing schedule (temperature, time and heating rate) and firing atmosphere are equally effective to attain ρ_{th} density of the sintered bodies. Improved forming process such as isostatic pressing and H_2 as sintering atmosphere will help to stop secondary grain growth to a greater extent of MAH doped alumina and it is possible to achieve ρ_{th} density. Difference in sintering behaviour of alumina with nature of addition of MgO (MAH or MN) may also introduce some change in material properties of the sintered pellets.

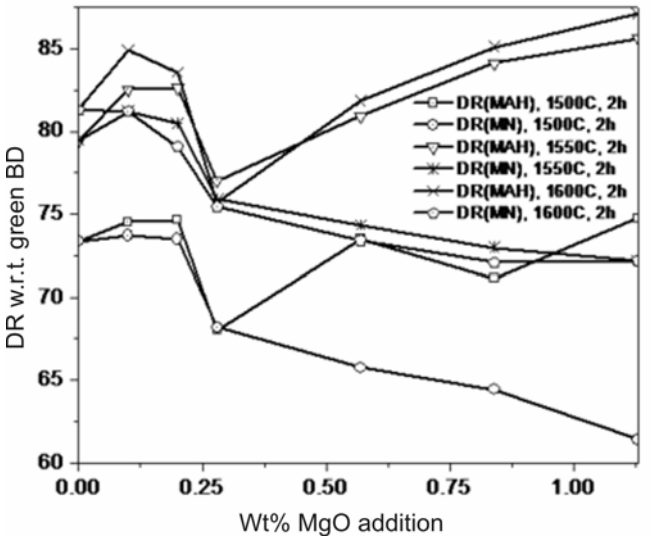

Figure 5. Effect of MgO addition as MAH/MN on DR with respect to green BD (loss free basis) during sintering of alumina.

3.3 *XRD analysis*

XRD curves of un-doped and MgO doped (MAH and MN) alumina samples sintered at 1600°C for 2 h have been depicted in figure 6. Un-doped alumina and alumina with up to 0·28 wt% addition of MgO in both the cases do not give clear evidence of peaks other than α-alumina (corundum). However, curves with 0·57 wt% MgO addition onwards in both the forms reveal magnesium aluminate spinel peaks with low relative intensity (RI).

Unit cell parameters '*a*', '*c*' and cell volume for all the compositions have been calculated based on major peaks of corundum (hexagonal) using standard relations (Cullity 1959) and incorporated in table 3. Significant increase in both unit cell parameters '*a*' and '*c*' has been observed when alumina is doped with MN. In case of doping by MAH, both unit cell parameters '*a*' and '*c*' have decreased marginally in some cases (0·1 and 1·13 wt% addition of MgO), otherwise their values have slightly increased. However, the increase in unit cell parameters is comparatively large in case of MN as source of MgO addition. Comparative % changes in '*a*', '*c*' and unit cell volume of sintered alumina with MgO addition (MAH and MN) have been incorporated in table 4. All values are with respect to un-doped α-Al_2O_3 and negative sign indicates a decrease.

Analysis of table 4 reveals that maximum % increase in unit cell volume for MAH doped sample is 0·5612, which is reasonably lower than MN doped samples where the value is 2·6743. Further, expansion of unit cell parameter '*a*' is almost double in 2D-plane than its perpendicular direction ('*c*'). In the previous work (Paul and Samaddar 1985), lattice contraction and expansion was reported in case of MgO addition as MAH up to 0·57 wt%, and for MN as 0·2 wt%. In the present work, purity of alumina is 99·9 wt% and XRD analysis has been carried out on a wide range of compositions. Both lattice contraction and expansion occur in MAH doped samples. Gradual increase in unit cell parameters for increasing amounts of both types of additions indicate solid solubility effect of MgO in alumina. However, spinel peaks appear with 0·57 wt% MgO addition onwards. Presence

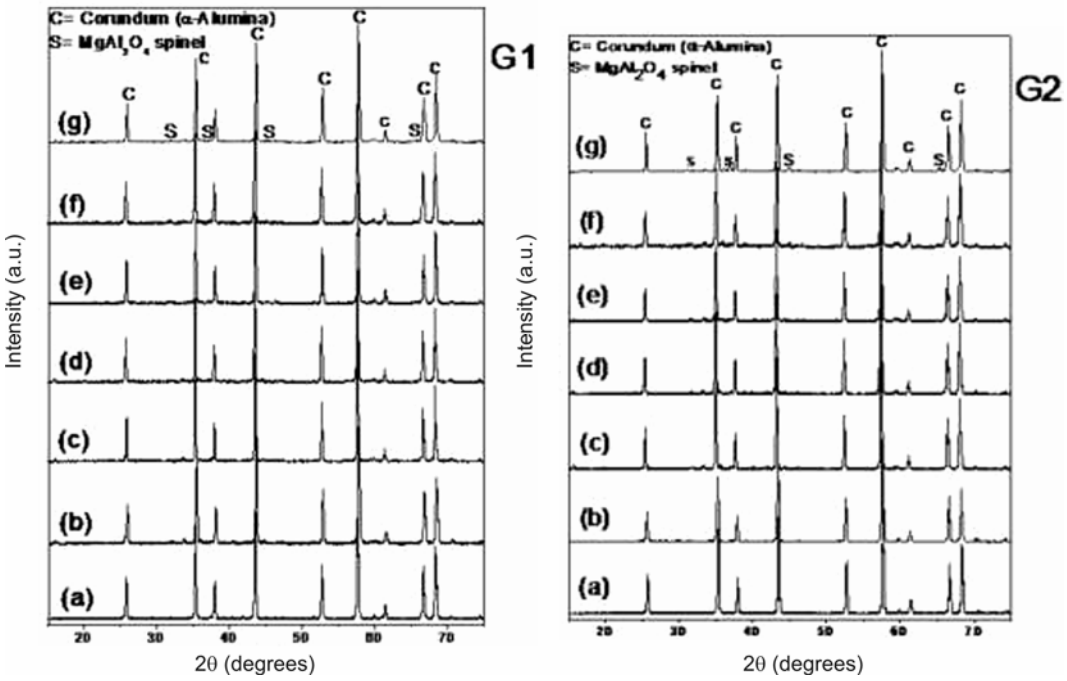

Figure 6. Comparison of X-ray curves of un-doped alumina with MgO additions as MAH (G1) and MN (G2). The $MgAl_2O_4$ (S) peaks have low intensity compared to α-Al_2O_3 (C). Here (a) un-doped alumina, (b) 0·1 wt% MgO, (c) 0·2 wt% MgO, (d) 0·28 wt% MgO, (e) 0·57 wt% MgO, (f) 0·84 wt% MgO and (g) 1·13 wt% MgO are shown.

Table 3. Effect of MgO (as MAH/MN) addition on unit cell parameters of sintered alumina.

Composition (wt% MgO addition)	Cell parameter, a (Å)		Cell parameter, c (Å)		Cell volume (Å^3)	
	MAH	MN	MAH	MN	MAH	MN
0·00	4·7387	4·7387	12·9656	12·9656	252·1417	252·1417
0·10	4·7338	4·756	12·9653	12·9806	251·6095	254·2744
0·20	4·7379	4·7783	12·9842	13·0300	252·4175	257·6516
0·28	4·7487	4·7828	12·9791	13·0260	253·4645	258·0590
0·57	4·7494	4·7892	12·9800	13·0329	253·5567	258·8847
0·84	4·7464	4·7810	12·9813	13·0206	253·2645	257·7527
1·13	4·7347	4·7577	12·9407	13·0232	251·2382	255·2973

Table 4. Effect of MgO (MAH/MN) addition on % change of unit cell parameters 'a', 'c' and cell volume of sintered alumina (corundum) at 1600°C, 2 h.

Composition (wt% MgO addition)	Change in a (%)		Change in c (%)		Cell volume change (%)	
	MAH	MN	MAH	MN	MAH	MN
0·10	–0·1034	0·3651	–0·0023	0·1157	–0·2111	0·8458
0·20	–0·0169	0·8357	0·1435	0·4967	0·1094	2·1852
0·28	0·2110	0·9306	0·1041	0·4658	0·5246	2·3468
0·57	0·2258	1·0657	0·1111	0·5191	0·5612	2·6743
0·84	0·1625	0·8926	0·1211	0·4242	0·4453	2·2253
1·13	–0·0844	0·4010	–0·1920	0·4443	–0·3583	1·2515

of spinel beyond optimum amount of MgO addition at grain-boundaries and grain corners of sintered alumina exerts stress on unit cell of alumina lattice, and causes gradual decrease in unit cell parameters and subsequently its unit cell volume. Effect is a maximum with 1·13 wt% addition of MgO both as MAH or MN.

In case of MAH addition, MAH forms spinel at much below the sintering temperature and then interacts with alumina during sintering. Structural coalescence of spinel with alumina within solid solubility limit of MgO in alumina may be the reason for decrease in unit cell parameters of alumina. For MN addition, MgO interacts with alumina during sintering where 3 Mg^{2+} ions with larger ionic radii replaces 2 Al^{3+} ions of smaller ionic radii. This causes increase in unit cell parameters and unusual expansion of unit cell volume of alumina.

3.4 *Microstructure interpretation*

Structural changes of alumina during sintering in presence of MgO have been reflected in the microstructures. In all the microphotographs of fractured surfaces, single and double black arrows indicate some of the inter-granular/intra-granular pores, whenever they appear. The precipitation of spinel phase on the edges, corners and surfaces of alumina grains have been marked with single and double white arrows. It is noteworthy to mention that in some microphotographs, very white patches appear at a few isolated places of fractured surfaces. These patches are not the same as indicated by the formation of spinel phase (in bright contrast) when the wt% addition of MgO is 0·57 and above. Figure 7 incorporates the microphotographs of un-doped and 0·1 wt% MgO (MAH and MN) doped alumina sintered at 1600°C, 2 h. There is no major difference in grain morphology of these samples. Many grains retain their initial identity i.e. grain surfaces are largely spherical and sharp edges/corners are absent. Only a small number of inter-granular pores can be seen in the photographs. Maximum (average) grain size achieved for un-doped alumina is ~2·49 μm, whereas the same for 0·1 wt% MgO sample is ~1·6 μm for both MAH and MN types. It is expected that addition of MgO will stop abnormal grain growth of alumina, though un-doped alumina does not show abnormal grain-growth mainly due to the use of submicron alumina powder and also fast cooling of sintered pellets.

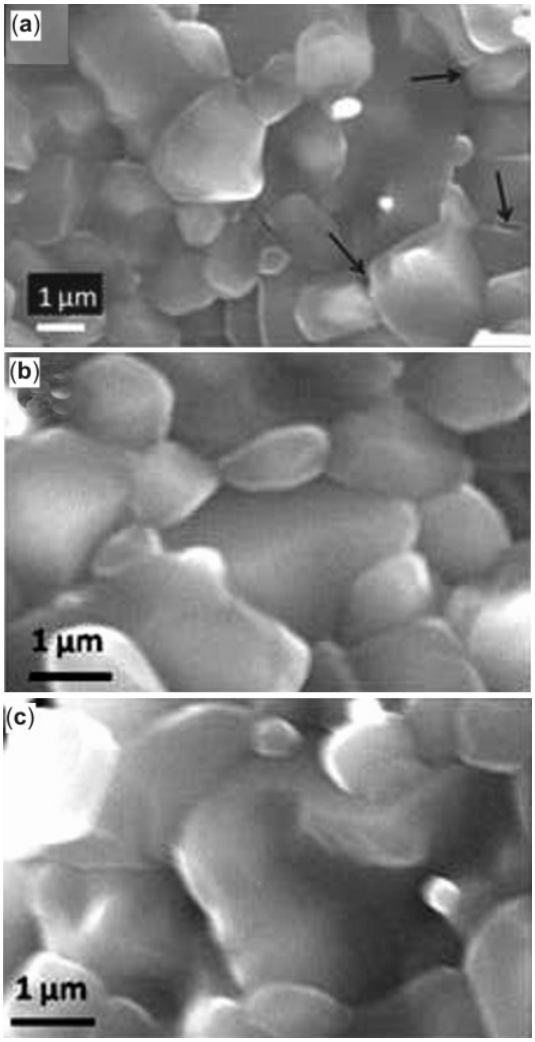

Figure 7. Scanning electron mode SEM images revealing similar grain morphology: (**a**) un-doped alumina, (**b**) 0·1 wt% MgO (MAH) and (**c**) 0·1 wt% MgO (MN) at 1600°C, 2 h.

Figure 8 reveals comparison of microstructures between MAH and MN doped alumina samples with wt% MgO addition as 0·2, 0·57, 0·84 and 1·13. There is distinct difference between microphotographs of 0·2 wt% MgO containing MAH and MN samples. In case of MAH (figure 8P1), identity of individual grains exists and their edges and faces are not very sharp. Normal grain-growth mostly occurs and average grain size is around 1·42 μm approximately. While inter-granular pores are visible at some places, intra-granular pores are negligible. For the MN doped sample (figure 8P2), there is normal grain growth, approximate average grain size is more (3·48 μm), edges are sharp but distorted and identity of individual grains is not clear.

One inference which can be drawn here is that when the addition of MgO exceeds its solid solubility limit in alumina, there is considerable change in microstructure. Figures 8Q1 and 8Q2 are for 0·57 wt% MgO doped alumina for MAH and MN, respectively. In both the cases grains have sharp edges and corners, and faces are quite flat. Precipitation of spinel as discrete particles in isolated places and also on edges/surfaces (along with the alumina grain) in both Q1 and Q2 suggests that MgO is present beyond its solid solubility limit. A few numbers of intra-granular pores are present in the microphotographs, and abnormal grain-growth with dense compact structure could be seen in both types of additions which have been interpreted to attain higher sintered densities as reported in §3·2.

Dense compact microstructure (figure 8R1) can also be achieved with 0·84 wt% addition of MgO as MAH, however, this compactness of grains is not visible when the addition is 1·13 wt% MgO as MAH (figure 8S1). Addi-

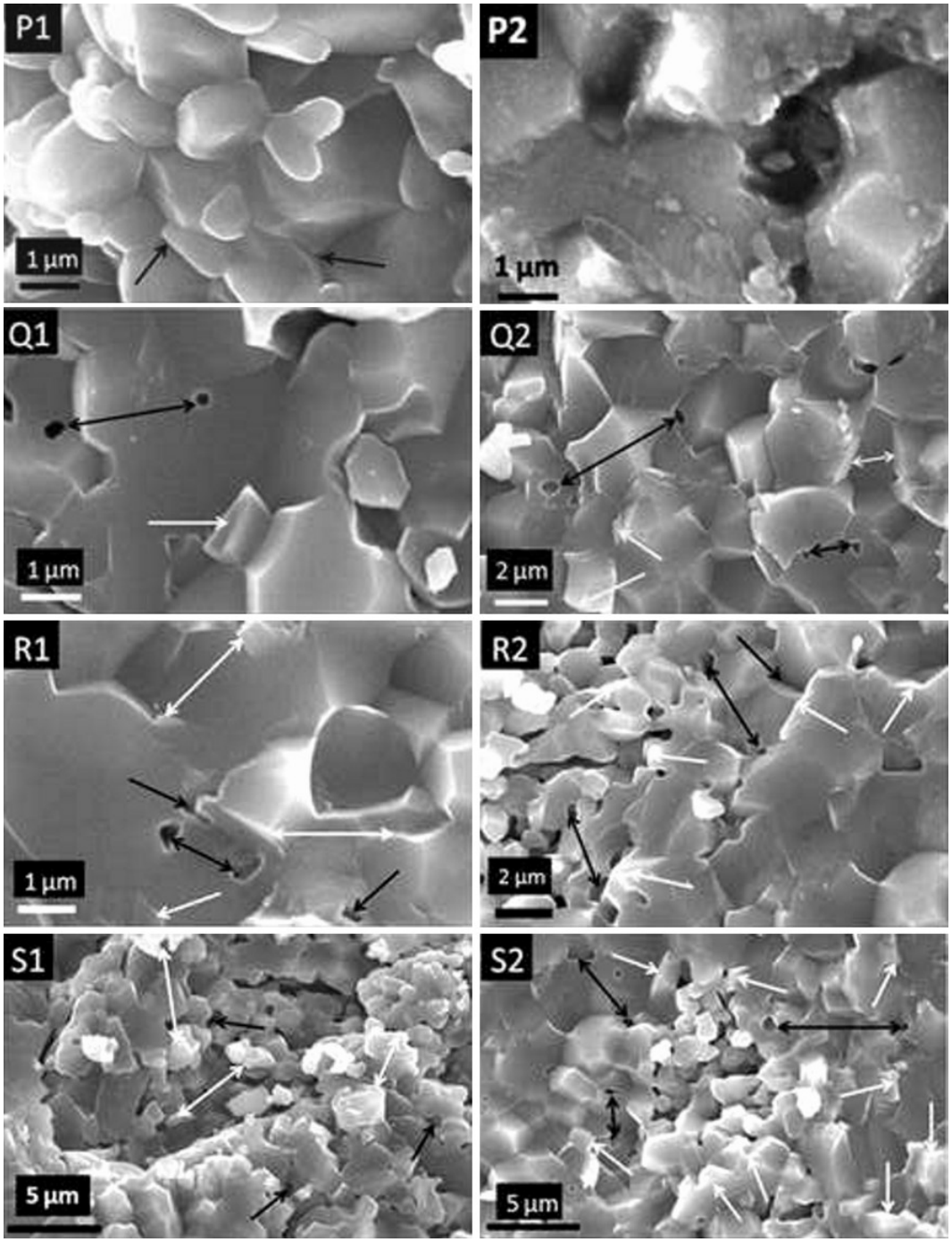

Figure 8. SEM images revealing comparative information regarding presence of inter or intra-granular pores and precipitation of $MgAl_2O_4$ spinel between specimens sintered at 1600°C, 2 h. (1) 0·2 wt% MgO as MAH (P1) and MN (P2); (2) 0·57 wt% MgO as MAH (Q1) and MN (Q2); (3) 0·84 wt% MgO as MAH (R1) and MN (R2); (4) 1·13 wt% MgO as MAH (S1) and MN (S2).

tion of 0·84 wt% MgO as MN evolves a cluster of small grains with large number of inter-granular voids (figure 8R2). But for 1·13 wt% MgO addition as MN, a dense compact mass of large grains with both intra and inter-granular voids is observed (figure 8S2). Microstructures of 1·13 wt% MgO addition pellets indicate better sintering i.e. higher BD and lower %A.P. and %T.P. in case of MN doped samples as compared to MAH (figures 1–3).

4. Conclusions

Based on the present investigation, the following major conclusions can be drawn:

(I) High purity submicron alumina powder compact prepared by unidirectional pressing can be sintered (in air) to near theoretical density with fine grain microstructure with hardly any intra-granular voids.
(II) Addition of MgO in alumina in either form (MAH or MN) has positive effect in densification to attain near ρ_{th} when it is added within optimum amount. MgO addition in the form of MAH is more effective as sintering aid than MN, and it is possible to achieve ~99% ρ_{th} with 0·28 wt% addition at 1550°C. For MN, the value is ~98% ρ_{th} at 0·2 wt% addition of MgO. Generation of intra-granular pores (closed pores) hinders further densification, and this effect is more when MgO is added in the form of MN as compared to MAH.
(III) XRD analysis indicates two types of structural changes of α-alumina depending on the nature of additions (MAH or MN). Unit cell volume of α-alumina gradually increases with addition of MgO and reaches a maximum value; however, further MgO addition reduces the cell volume. For MN type of addition, maximum unit cell volume is attained at 0·57 wt% MgO. In case of MAH, it is at 0·28 wt% MgO.
(IV) Solid solution of MgO in alumina and its segregation as spinel may drag pores so that spinel exists more as discrete particles at grain corners than along edges of grains and grain boundaries.

Acknowledgement

Financial support of this work was provided by Technical Education Quality Improvement Program (TEQIP) Fund of Govt. College of Engineering & Ceramic Technology, Kolkata.

References

Cahoon H P and Christerson J 1956 *J. Am. Ceram. Soc.* **39** 337
Coble R L 1961 *J. Appl. Phys.* **32** 793
Coble R L 1962 U.S. Patent 302610
Cohen Abraham, Van der Merwe C P and Kingon A I 1984 in *Advances in ceramics* (ed.) W D Kingery (Ohio, Columbus: Am. Ceram. Soc. Inc.) **Vol. 10** pp 780–790
Cullity B D 1959 *Elements of X-ray diffraction* (USA: Addison-Wesley Publishing Company, Inc.) p. 309
Haroun N A and Budworth D W 1970 *Br. Ceram. Trans.* **69** 73
Johnson W C and Coble R L 1978 *J. Am. Ceram. Soc.* **61** 110
Jorgensen P J 1965 *J. Am. Ceram. Soc.* **48** 207
Jorgensen P J and Westbrook J H 1964 *J. Am. Ceram. Soc.* **47** 332
Li C W and Kingery W D 1984 in *Advances in ceramics* (ed.) W D Kingery (Columbus, Ohio: Am. Ceram. Soc. Inc.) **Vol. 10** pp 368–378
Mukherjee S G and Samaddar B N 1969 *Indian J. Chem.* **7** 183
Paul P G and Samaddar B N 1985 *Trans. Ind. Ceram. Soc.* **44** 132
Samaddar B N, Paul P G and Bhattacharyya Hemanta 1979 *Trans. Ind. Ceram. Soc.* **38** 151
Smothers W J and Reynolds H J 1954 *J. Am. Ceram. Soc.* **37** 588
Taylor R I, Coad J P and Brook R J 1974 *J. Am. Ceram. Soc.* **57** 539
Taylor R I, Coad J P and Hughes A E 1976 *J. Am. Ceram. Soc.* **59** 374
Warman M O and Budworth D W 1967 *Br. Ceram. Trans.* **66** 253